Pramāṇa, Vol. 23, No. 1, July 1984, pp. 1–16. © Printed in India.

# Rotating relativistic electron beam-plasma interaction and formation of a field-reversed configuration

K K JAIN and P I JOHN

Plasma Physics Programme, Physical Research Laboratory, Ahmedabad 380009, India

MS received 16 April 1984

**Abstract.** Experimental results on interaction of a rotating relativistic electron beam with plasma and neutral gas are presented. The rotating relativistic electron beam has been propagated up to a distance of 150 cm in a plasma. The response of the plasma to the rotating electron beam is found to be of magnetic diffusion type over a plasma density range $10^{11}$–$10^{13}$ cm$^{-3}$. Excitation of the axial and azimuthal return currents by the rotating beam and subsequent trapping of the azimuthal return current layer by the magnetic mirror field are observed. A field-reversed configuration has been formed by the rotating relativistic electron beam when injected into neutral hydrogen gas. We have observed field reversal up to three times the initial field in an axial length of 100 cm.

**Keywords.** Relativistic electron beam; return current; plasma heating; field-reversed configuration.

PACS No. 52·60

## 1. Introduction

Recent technological advances have placed at our disposal intense relativistic electron beam (REB) devices capable of delivering MJ energy in sub-$\mu$ sec time scales. These intense electron beams have been used for flash x-ray production and material studies (Oswald *et al* 1966), to excite high pressure gases (Bagratashoili *et al* 1973), for high power microwave generation (Nation 1970) and collective ion acceleration (Graybill and Uglum 1970).

Relativistic electron beams can be used for direct heating of a high density plasma to high temperatures. In laminar electron beam-plasma interaction, the experimental results have shown that optimum energy transferred from the beam to the plasma takes place at $n_p = n_b$ (where $n_p$ is the plasma density and $n_b$ is the beam density). At a plasma density much higher than the beam density, the energy coupling efficiency falls drastically. Chu and Rostoker (1974) suggested a new scheme which is characterised by a relatively high coupling efficiency at $n_p \gg n_b$. The method suggested was to use a rotating electron beam in place of the laminar beam. In rotating electron beam—plasma interaction, transfer of beam energy to the plasma can occur not only through excitation of microturbulence, but also via other mechanisms such as electrostatic acceleration of ions by the equilibrium electric field (Chu and Rostoker 1974; Molvig and Rostoker 1977a), excitation of magnetosonic waves (Chu *et al* 1975; Molvig and Rostoker 1977b) and also joule heating.

The first experiment on rotating beam-plasma interaction was performed by Kapetanakos *et al* (1975a) to study the dependence of energy transfer on plasma density. The optimum energy transfer was observed at a plasma density, two orders of

magnitude greater than the beam density. The rotating electron beam-plasma interaction through magnetic perturbations and radial oscillations was studied by Roberson (1978). Field reversal configuration created by the induced plasma currents was observed in this experiment. An attempt was made to compare the braking of the beam with existing theoretical models and magnetic perturbations with numerical calculations. Another important advantage of the rotating electron beam over laminar one is that the rotating beams are capable of creating a reverse magnetic field configuration and a plasma confined in such a configuration of fields is known to be stable against MHD instabilities. This field reversal configuration with closed field lines exhibits favourable confinement properties for high $\beta$ plasmas. The availability of high power electron beam generators has made it possible to produce field reversal in a single pulse (Andrew *et al* 1971). Reverse field, created by the rotating beam induced plasma currents, has been observed when injected into an initially neutral gas (Kapetanakos *et al* 1975b; Sethian *et al* 1978a; Roberson *et al* 1978). Field-reversed configuration even in the absence of external magnetic field has been observed recently (Sethian 1978b).

In this paper, we present experimental results on interaction of a rotating electron beam with a magnetically confined plasma and generation of field reversed configuration. The experimental device and associated diagnostic elements used in the course of the investigation are described in §2. Experimental and numerical results to study the rotating relativistic electron beam-plasma interaction are presented in §§3 and 4 respectively. In §5 observational evidences for the generation of a field-reversed configuration by the rotating electron beam when injected into neutral gas are presented. The experimental results of §§3 and 5 are discussed in §6. The main results of this paper are summarised in the last section.

## 2. Experimental device and diagnostics

A schematic of the experimental set-up along with key diagnostics and magnetic field configuration is shown in figure 1. The experimental device consists of a vacuum chamber, a system of magnetic field coils, a plasma gun and a relativistic electron beam generator. The vacuum chamber is a 30 cm diameter, 2·3 m long stainless steel tube evacuated to a base pressure of $10^{-5}$ torr using vapour diffusion pumps. The magnetic field configuration is a combination of a mirror and a nonadiabatic cusp field. The pancake magnetic field coils, connected in series and placed over the SS chamber, are energised by a 8 kJ condenser bank. The magnetic field configuration has a mirror ratio of 2·6 and a mirror to mirror distance of 125 cm. The nonadiabatic cusp field is produced by reversing the direction of the current in the first three coils of the magnetic field assembly. A 25 mm thick mild steel annular plate is introduced between the two sets of coils. An additional set of coil is wound directly over the chamber in order to make the cusp strongly nonadiabatic. During the field-reversed experiments, some coils of the magnetic field assembly were shorted so that after the cusp, magnetic field is homogeneous instead of having mirror configuration.

A modified version of the washer gun, in which gas is injected externally is used as a plasma source (Jain *et al* 1980). The plasma gun consists of a number of brass and nylon washers with an inner diameter of 22 mm and thickness of 5 mm stacked together alternately. The first washer acts as a cathode and the last is connected to the ground

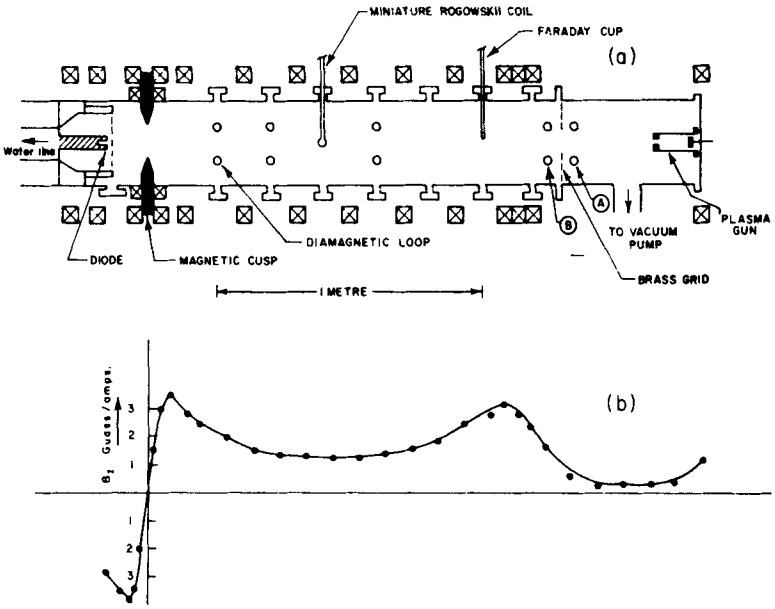


**Figure 1.** Schematic of the experimental set-up and magnetic field profile.

through metallic rods. The gas to be ionised is let into a nylon plenum using a slow pulsed electromagnetic valve and enters near the cathode. The gun is powered by an eight-stage pulse forming line, consisting of 5 $\mu$F low inductance capacitors and 2·4 $\mu$H inductors. Hydrogen plasma of typical density $10^{11}$–$10^{13}$ cm$^{-3}$ has been obtained from this gun.

The relativistic electron beam generator consists of a Marx generator, co-axial water line, high voltage holding switch (self-triggered water switch) and a field emission vacuum diode (Jain and John 1981). A high voltage power supply charges a Marx generator. On a trigger command, the Marx is erected by switching all the capacitors in series and thus providing the high voltage needed. Next, the stored energy is transferred in less than a $\mu$sec to co-axial water line that enables a time-compression of the voltage pulse. The beam generation and acceleration occurs in the beam diode, which is energised by the water line. The diode consists of an annular brass cathode of 40 mm o.d., 26 mm i.d. and in front of it, is placed an anode of 6 $\mu$m thick aluminium foil. A 200–250 keV, 10–15 kA, 80 nsec duration electron beam has been obtained. Rotation is imparted to the beam by the nonadiabatic cusp when the beam crosses it.

Diagnostics deployed to study the rotating REB-plasma interaction and field-reversed configuration were Langmuir probes, Faraday cups, witness plates, 22 GHz microwave interferometer and an energy selective electron probe. A miniature Rogowskii coil and an array of diamagnetic loops were constructed specifically to study the net currents and beam induced magnetic field. The energy selective electron probe is made of a cylindrical SS disc (or wire) of 5 mm diameter covered with a 6 $\mu$m thick aluminium foil capable of preferentially collecting energetic electrons (Jain 1982).

## 3. Rotating REB-plasma interaction

### 3.1 *Beam propagation*

A series of measurements have been made to study the propagation of the rotating electron beam through plasma. These studies were carried out using an array of identical diamagnetic loops placed at different axial distances, two energy selective electron probes and a Faraday cup. When the beam was fired in vacuum, the diamagnetic loop and Faraday cup registered the beam only up to a distance of 25 cm from the cusp. While studying the rotating beam propagation through plasma, the chamber was filled with hydrogen plasma (density $\approx 10^{12}\,cm^{-3}$) produced by the plasma gun. All the diamagnetic loops including the one placed outside the second mirror (loop-B) registered the rotating beam induced signals. The energy selective electron probe placed at the mirror minimum region, used for determining the life time of the beam in the mirror, showed (figure 2) that a substantial part of the beam induced signal lasts for only 100 nsec, which is comparable to the beam pulse length, although the overall extent of the signal is about 250 nsec. These results show that the presence of plasma leads to an efficient propagation of the beam all along the chamber.

We have observed a large variation of magnetic field ($\Delta B/B_0 = 0{\cdot}7$, $\Delta B$ is the beam induced field and $B_0$ is the external field) near the end brass grid as compared to the signals recorded at other axial positions, as shown in figure 3a. This large signal is attributed to the piling up of rotating beam particles near the brass grid after traversing through the plasma. This is confirmed by the diamagnetic loop A placed on the other side of the grid, which registers a comparatively small signal, as seen from figure 3b.

### 3.2 *Net axial and azimuthal currents*

A miniature Rogowskii coil deployed at 65 cm from the cusp plane and at a radial distance of 20 mm from the axis, was used to monitor the net currents. Its axis was oriented parallel to that of the system to enable it to register the axial component of the

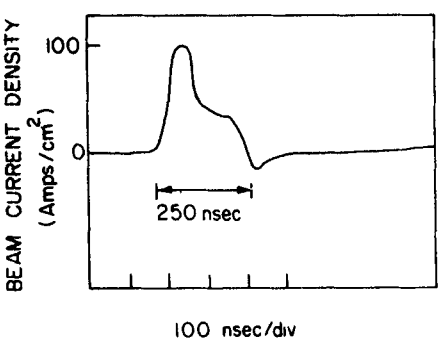


**Figure 2.** Electron beam current density, measured with an energy selective electron probe at the mirror centre.

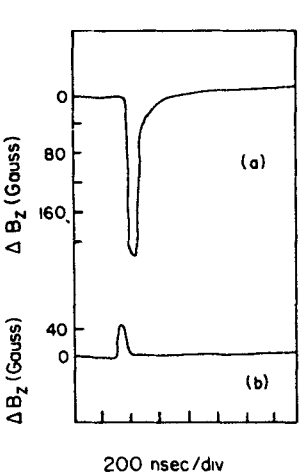


**Figure 3.** The diamagnetic loop output measured (**a**) at the inner side of the grid with loop B, (**b**) at a point outside the grid with loop A.

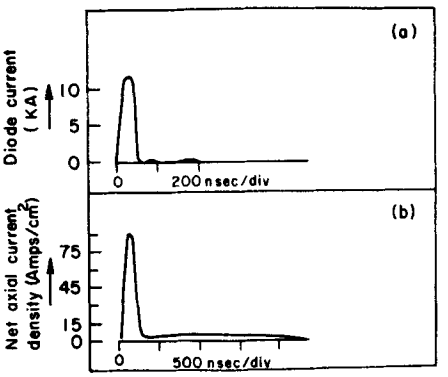


**Figure 4.** (a) A typical diode current output (b) Net axial current density as function of time obtained at 20 mm radial position.

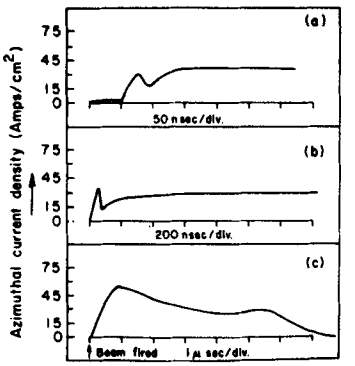


**Figure 5.** Time evolution of the net azimuthal current.

net currents. Figure 4 depicts a typical net axial current monitored by the Rogowskii coil. The positive signal corresponds to currents, flowing in the same direction as that of the beam propagation. The net axial current peaks at 100 nsec with a current density equal to 100 A/cm$^2$. Figure 4 also shows that substantial part of the net axial current lasts for a period much longer than the beam duration.

During the net azimuthal current measurements, the machine was operated in the same parameter range as in net axial current. The miniature Rogowskii coil was rotated by 90° so that its axis was perpendicular to the system axis. Figure 5 shows the time evolution of the net azimuthal current registered by the coil for three different time scales. The positive signal corresponds to the net azimuthal current flowing in the same direction as the beam rotation. The net azimuthal current starts building up only after 50 nsec and reaches the peak value of 60 A/cm$^2$. Absence of appreciable amount of current during the beam duration (*i.e.* initial 50 nsec) indicates that the beam is azimuthally current neutralised to a good extent. The total net azimuthal current lasts for nearly 6 $\mu$sec. By comparing figures 4b and 5, we note that the net axial current builds up quite fast and decays also rapidly, in contrast to the net azimuthal current which increases slowly and decays at an even slower rate. The amplitude of the net axial current is larger than the azimuthal one, but its life time is shorter by an order of magnitude.

The radial profile of the net axial and azimuthal current was obtained by moving the Rogowskii coil radially. It was found that both the currents peak at a radial distance of 20 mm (Jain 1982) which is the radial position of the beam. Time profiles of the currents do not change significantly as the coil is moved radially. In both cases, some finite currents do exist even at a distance of 90 mm from the axis.

By knowing the net azimuthal current density at various points along the radius and length of this current layer (see §3.3), radial profile of the induced axial magnetic field is obtained, as shown in figure 6. We observe that the induced axial magnetic field is diamagnetic up to a radial distance of 25 mm from the axis, having a peak value of 140 Gauss. This $\Delta B$ value obtained in the mirror minimum region corresponds to a reduction of external magnetic field by 45 %. The induced axial magnetic field changes polarity, *i.e.*, becomes paramagnetic after a distance of 25 mm from the axis.

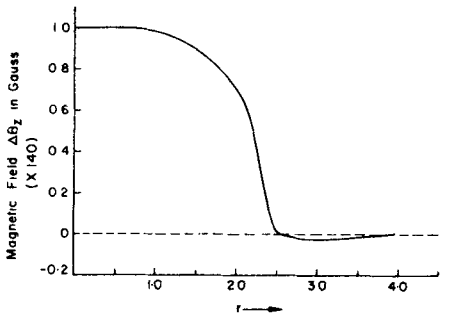


**Figure 6.** Radial profile of the beam induced axial magnetic field.

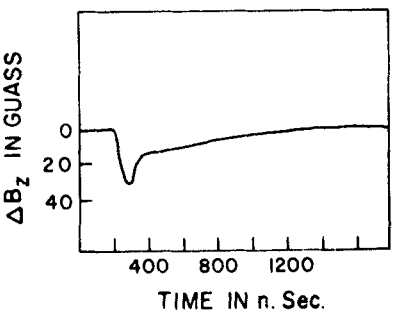


**Figure 7.** A diamagnetic loop output showing the magnetic perturbation at the mirror centre as a function of time.

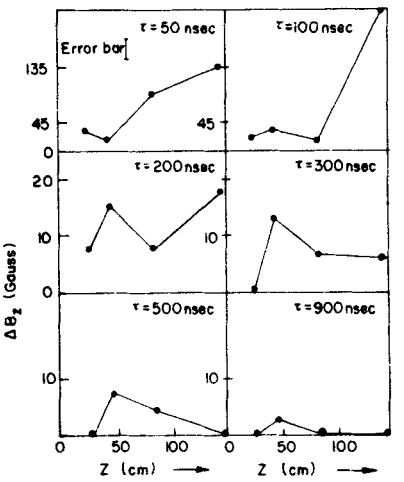


**Figure 8.** Spatial behaviour of magnetic perturbation at different intervals of time. The horizontal axis represents the distances marked from the cusp plane. The mirror centre is at 70 cm, and grid at 155 cm.

### 3.3 *Azimuthal current layer*

The magnetic response of the plasma to the rotating beam was monitored using an array of identical diamagnetic loops kept at different axial locations encircling the plasma. The diamagnetic loops were calibrated using a pulsed magnetic field produced by a 35 A, 100 nsec square current pulse generated by a co-axial cable pulse forming line discharging into a single turn loop in series with a matched load. The output of the diamagnetic loops was recorded on storage oscilloscopes as a function of time and later collated to study the spatial and temporal behaviour of magnetic perturbations. The problems due to the shot to shot variations, common to many intense pulsed beam experiments were partially taken care of by using the loop located at the mirror centre as a standard.

The magnetic perturbation at the mirror centre reaches a maximum in 100 nsec and then begins to decay (figure 7). The relatively fast rise and slower decay is characteristic of signals from all loops kept within the mirror. The spatial behaviour shows the following significant aspects (figure 8). After 100 nsec of the beam injection, the signals

all along the region from the cusp to the wall begin to decrease. After 300 nsec the signals near the cusp and near the wall, both outside the mirror, reduce to zero while the signal at the centre of the mirror is seen to persist. An axially movable diamagnetic loop is used to study the behaviour at the central region where the signals typically last for times of the order of a $\mu$sec. The length of the column where persisting signals are seen is about 60 cm and is symmetrically located around the mirror centre. As time progresses the spatial extent shrinks axially.

The possibility that the persisting diamagnetic signal was due to trapping of the energetic electrons in the mirror can be ruled out by the fact that the diamagnetic loops located outside the mirror throat and near the wall showed a 300 nsec signal, indicating that the rotating beam did cross the mirror. To corroborate this further, an energy selective electron probe was used to drain off the energetic electron current. Even then the signal obtained from the diamagnetic loop remained qualitatively the same, with the long persistence time showing that we are indeed observing the signal due to the azimuthal current induced in the plasma by the beam.

The observation of persisting diamagnetic currents after the beam has escaped from the mirror and its spatial restriction to regions inside the mirror indicates that this region is isolated electrically from the walls. We have confirmed this by observing that the parallel currents, excited by the parallel component of the beam current persists only in the beginning when the plasma all along the beam path shows diamagnetic behaviour. After 300 nsec when the diamagnetic behaviour is confined to the region within the mirror the axial current monitored using a Rogowskii coil reduced considerably.

The dependence of the diamagnetic loop signal on the plasma density was studied by firing the beam generator at different time delays with respect to the plasma gun discharge, thus corresponding to different plasma densities. The plasma density attains a peak value of $10^{13}$ cm$^{-3}$ at time delays of 200 $\mu$sec. For delays smaller or larger than 200 $\mu$sec the plasma density decreases. From figure 9, we observe that with a decrease in the plasma density, the strength of the loop signal also decreases. Further, the dependence of the diamagnetic loop signal on the external magnetic field at the mirror centre was also studied. As shown in figure 10, the loop signal peaks at a value of 900 Gauss at the mirror point which corresponds to the observed cusp cut-off magnetic field (Schmidt 1962) for 200 keV REB.

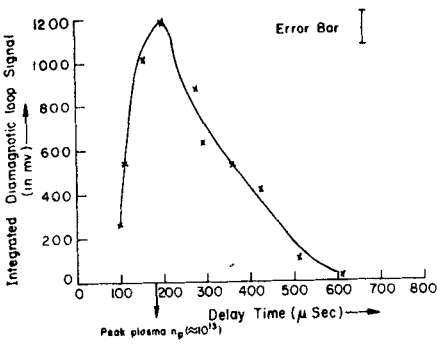


**Figure 9.** Dependence of the peak diamagnetic loop signal on the time delay between the beam generator and the plasma gun firing.

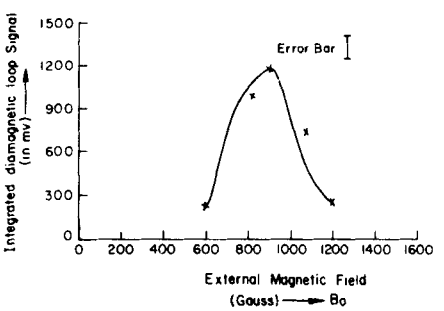


**Figure 10.** Dependence of the peak diamagnetic loop on the external magnetic field. Horizontal axis represents the field at the mirror point.

## 4. Numerical studies on the magnetic response of the plasma

We present in this section numerical results of the temporal behaviour of return and net azimuthal current. These results are obtained using a magnetic diffusion model. Since no radial plasma oscillations are observed in our experiment, use of the magnetic diffusion model is justified. The beam current has been modelled as an infinitely long, thin annular current sheet of radius 2 cm embedded in a cylindrical plasma column of radius 4 cm.

The return and net azimuthal current which are proportional to the azimuthal electric field $E_\theta$ and axial magnetic field $B_z$ respectively, can be obtained by solving diffusion equation for vector potential $A_\theta$ (see for details, Striffler and Kapetanakos 1975), *i.e.*,

$$\frac{\partial}{\partial r}\frac{1}{r}\left(\frac{\partial}{\partial r} rA_\theta\right) - \mu\sigma^* \frac{\partial A_\theta}{\partial t} = 0,$$

(where $\sigma^*$ is effective conductivity of the plasma) and introducing it into

$$B_z = \frac{1}{r}\frac{\partial}{\partial r} rA_\theta,$$

$$E_\theta = -\frac{\partial A_\theta}{\partial t}.$$

A triangular beam current pulse $I(t)$ as a function of time was chosen to solve the diffusion equation. Figures 11 and 12 depict azimuthal electric field which is essentially proportional to the angular return current at various radial positions. At $R = 2$ cm *i.e.* at the beam radial position we observe that at low conductivity, there is sharp rise and fall of the $E_\theta$, in time which decreases as the conductivity increases. The peak amplitude of return current decreases rapidly with increase in conductivity. There is change of sign of electric field $E_\theta$ and hence that of the return current after the beam pulse duration. The negative signal corresponds to flow of azimuthal return current in a direction opposite to the beam while positive signal corresponds to same direction as the beam rotation. There is no delay between the peak value at various $\sigma^*$ for $R = 2$ cm. But at

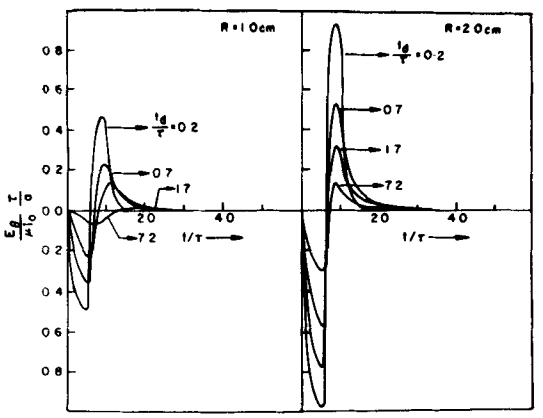


**Figure 11.** Azimuthal electric field as function of time for different conductivities within the beam radius. Here $\tau$ is the beam pulse duration, $\tau_d = 4\pi\sigma^* a^2/c^2$, $a$ is the beam radius, $I_0$ is the peak beam current per unit length.

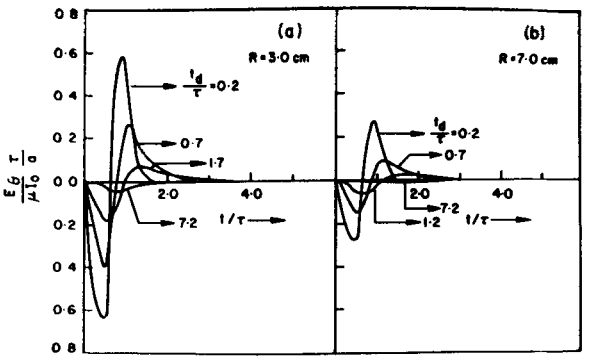


**Figure 12.** Azimuthal electric field as function of time for different conductivities outside the beam cross-section.

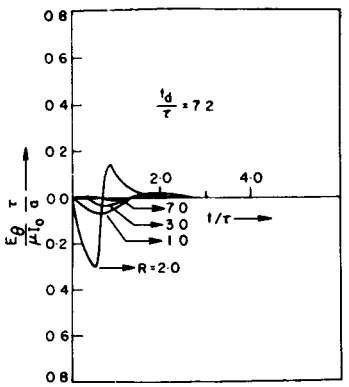


**Figure 13.** Time variation of the azimuthal electric field at different radius.

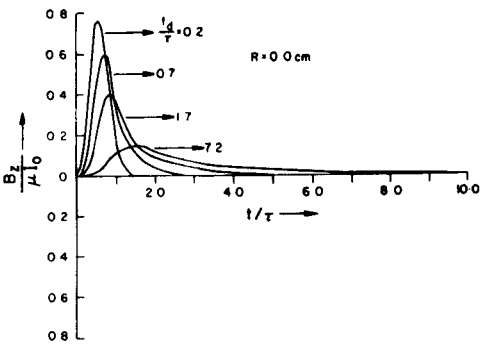


**Figure 14.** Dependence of the induced axial magnetic field at the axis on plasma conductivity.

other radial positions, there is a delay between the peaks which increases with conductivity. From figure 12, we observe some finite return current even at a radial distance of 7 cm. The beam-induced azimuthal return current peaks at 2 cm, however at higher values of $\sigma^*$, most of the current is localised at $R = 2$, as is evident from figure 13.

Figure 14 shows the axial magnetic field which is proportional to the net angular current, at the centre. For $\sigma^* = 0$, the magnetic field is identical in shape to the beam pulse. The amplitude of the signal decreases with conductivity. For higher conductivities the magnetic field peaks after the pulse is over. Also decay time of the net angular current increases with $\sigma^*$. At $R = 1$ cm, the magnetic field is always diamagnetic while at 3 cm radial distance (figure 15), the first signal is paramagnetic and then it is diamagnetic.

## 5. Generation of field reversed configuration

Recently, there has been considerable interest on the formation of compact torii, which is an axisymmetric magnetic confinement system in which poloidal ($B_z$) field lines are

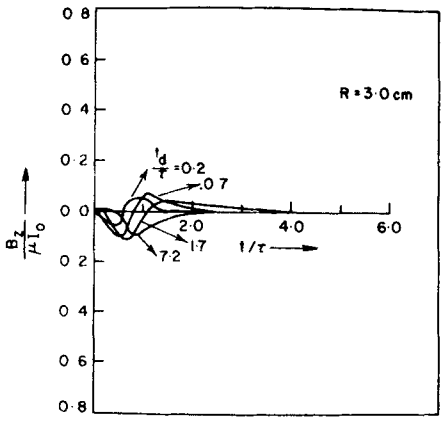


**Figure 15.** Induced axial magnetic field's time profile at 30 mm radius.

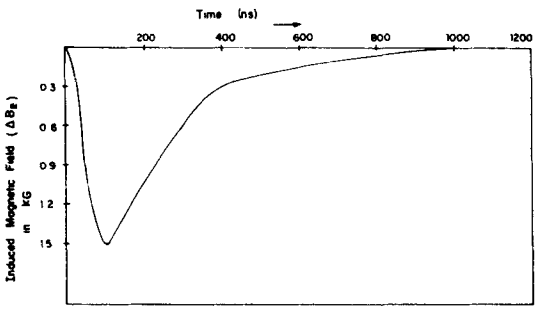


**Figure 16.** Time evolution of the diamagnetic loop when rotating electron beam is injected into neutral gas.

closed and encircle the plasma while toroidal field ($B_\theta$) is trapped within the plasma. Compact torii have been created by field-reversed theta pinch technique (Armstrong *et al* 1981; Es' Kov *et al* 1978), by trapping poloidal flux in fast moving plasma ring ejected by co-axial type plasma gun (Jarboe *et al* 1980) and by electron layer in the Astron device (Rej 1981). A novel method using rotating relativistic electron beam (REB) has been suggested to produce a compact toroid (Sethian *et al* 1982) which requires generation of field-reversed configuration, reconnection of antiparallel field lines at two ends and reversal of the axial current on the plasma surface or its dissipation within Alfven time. In this section, we present experimental results on formation of a field reversed configuration by a rotating electron beam.

The experimental set-up and magnetic field configuration have been slightly modified from the one used for rotating REB-plasma interaction studies. After the magnetic cusp, the magnetic field configuration was made homogenous. In this series of experiments, the vacuum chamber was filled with neutral hydrogen gas in the 30–300 m torr pressure range. The beam generator was operated in 200–250 keV, 10–15 kA, 100 nsec parameter range. Immediately after leaving the field emission diode, the electron beam passes through a 6 $\mu$m thick aluminium foil which maintains the pressure difference between diode region (pressure $\sim 10^{-5}$ torr) and the main vacuum chamber, containing hydrogen gas at a pressure of few hundred m torr. The induced

magnetic fields are measured by an array of spatially dispersed diamagnetic loops and a magnetic probe.

Temporal variation of the rotating relativistic electron beam induced axial magnetic field measured with diamagnetic loop at an axial distance of 22 cm from the cusp plane and at 300 m torr pressure is shown in figure 16. The induced magnetic field peaks to a value of 1·5 kG in 100 nsec and lasts for 1 $\mu$sec. This peak value of $\Delta B_z$ corresponds to three times the initial magnetic field or in other words, axial magnetic field is completely reversed ($\Delta B_z > -2B_0$, $B_0$ is the initial external magnetic field). Magnetic probe signals monitored on and off the axis are depicted in figure 17. The on-axis induced magnetic field is diamagnetic while off-axis is paramagnetic. Further, on the axis, induced magnetic field is larger by an order of magnitude as compared to the off-axis field.

Dependence of induced magnetic field $\Delta B_z$ on background neutral gas pressure is studied. The strength of the reversed field peaks at 300 m torr pressure as shown in figure 18. This behaviour indicates that at 300 m torr pressure, charge neutralisation of the rotating electron beam is maximum while current neutralisation is minimum. Experimental results on dependence of the induced magnetic field $\Delta B_z$ on the initial

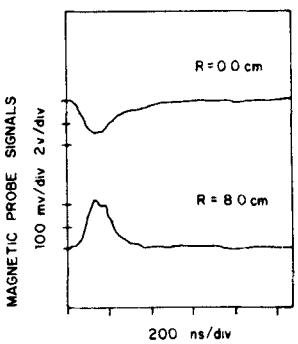


**Figure 17.** Magnetic probe output on and off axis.

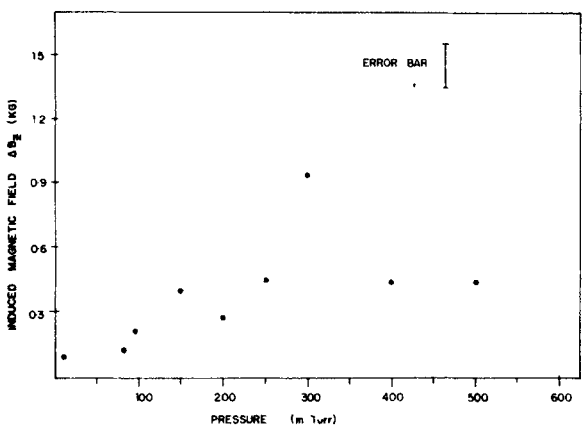


**Figure 18.** Variation of the induced axial magnetic field with neutral gas pressure.

magnetic field are contrary to the observations of Roberson *et al* (1978). We observe increase in $\Delta B_z$ with the initial magnetic field (figure 19).

Spatial dependence of $\Delta B_z$ is studied using an array of identical diamagnetic loops located at different axial positions. The shot-to-shot variation was taken into account by using one of the diamagnetic loops as a standard. Figure 20 shows the axial dependence of the peak value of induced magnetic field $\Delta B_z$. The length of the field reversed configuration is about 100 cm, longer by a factor of two as compared to results reported in other experiments (Sethian *et al* 1978a; Roberson *et al* 1978). At the centre, the strength of the field reversal is more by a factor of two as compared to that at ends. This spatial behaviour can be explained by visualising the current carrying plasma layer as a solenoid.

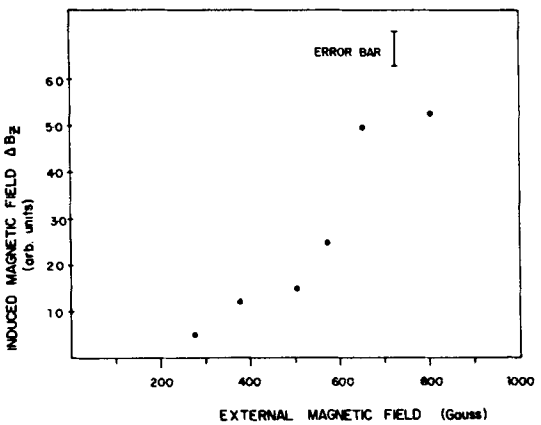


**Figure 19.** Dependence of the beam induced axial magnetic field $\Delta B_z$ on the external magnetic field $B_0$.

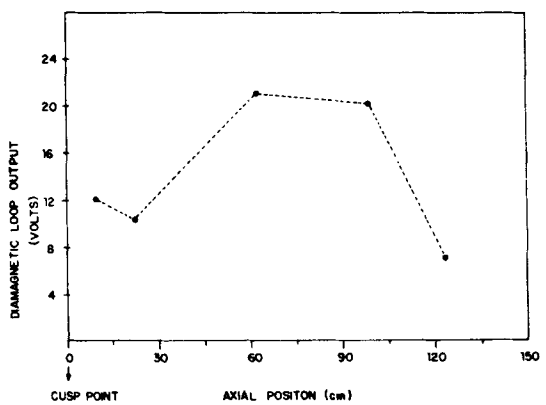


**Figure 20.** Spatial variation of induced magnetic field along the system length.

## 6. Discussion

### 6.1 *Beam propagation characteristics*

Molvig and Rostoker's (1977a) magnetic diffusion model has predicted the generation of azimuthal return current in addition to the usual axial return current when rotating electron beam is injected into plasma. They have shown that the subsequent decay of these counter flowing plasma currents can produce an efficient retarding force on the beam. The stopping length of the rotating beam thus calculated is:

$$l_s = \frac{1}{2}\frac{n_p}{n_b}\left(\frac{V_\parallel}{c}\right)^3 \frac{\gamma}{\nu_e},$$

where $n_p$ is the plasma density, $n_b$ the electron beam density, $V_\parallel$ is the axial plasma velocity and $\gamma$ is the relativistic mass factor.

The collision frequency $\nu_e$ is a difficult parameter to measure during the interaction. Hence it has been determined by comparing the rising part of the observed diamagnetic loop signal with that of numerical calculations using a diffusion model (for details see Jain 1982). The $\nu_e$ value thus obtained is $10^7\ \text{sec}^{-1}$. For $n_p = 10^{13}$, $n_b = 10^{11}$, $V_\parallel = 10^{10}$ cm/sec, $r = 1{\cdot}4$, the stopping length turns out to be a few meters, much longer than the length of the vacuum chamber, as observed in our experiment.

The accumulation of the rotating electron beam near the end brass grid could be explained in the same way as $E$ layer trapping using resistive rings in the ASTRON machine. It has been shown by Nabenzahl (1973) that a rotating electron beam, passing through a resistive ring, induces an azimuthal current in the ring and the fields produced by the induced currents interact with the beam electrons. The energy dissipation as heat in the resistive ring is at the cost of the beam's axial energy alone while rotational energy of the beam remains unchanged. In the present experiments, when the rotating electron beam approaches the brass grid, azimuthal counter currents are induced in the conducting grid. These induced currents interact with the beam and as a result the beam slows down causing piling up of the beam particles.

### 6.2 *Magnetic response of plasma*

The magnetic diffusion model by Chu and Rostoker (1974) and Molvig and Rostoker (1977a) deals with the physical mechanism for the generation of axial and azimuthal return currents and also the effect of decay of these currents on the rotating beam itself. It has been shown that axial return current results due to the induced electric field $E_z$ and due to the rotation of the electron beam, electric field $E_\theta$ and as a consequence of $E_\theta \times B_z$ drift of electrons, radial electric field $E_r$ is created. The radial electric field $E_r$, leads to an azimuthal return current through the $E_r \times B_z$ drift of plasma electrons. However, in cases when plasma ions are magnetized, the dominating mechanism for the generation of azimuthal return current is of the resistive type i.e. $J_\theta = \sigma^* E_\theta$.

For our initial experimental parameters $T_e = 5$–$10$ eV, $n_p = 10^{12}\ \text{cm}^{-3}$ the electron and ion collision frequencies are equal to $10^6\ \text{sec}^{-1}$ and $10^4\ \text{sec}^{-1}$ respectively. The electron and ion cyclotron frequencies at the mirror minimum are $5 \times 10^9\ \text{sec}^{-1}$ and $3 \times 10^6\ \text{sec}^{-1}$ respectively. Thus, in the present experiment, both electrons and ions being magnetised, the azimuthal return current will be driven dominantly by azimuthal electric field $E_\theta$ rather than by $E_r \times B_z$ drift of electrons. Experiments were conducted

for further verification whether $E_r \times B_z$ is the mechanism for the generation of the observed return currents. An electron multiplier placed in the system to register any fast ions or charge exchanged neutral flux which should be a natural consequence if $E_r$ is generated as per the model, did not detect any ion or neutral particles.

The experiments conducted to verify the dependence of the diamagnetic loop signal decay time on the mass of the plasma ions also did not give the expected dependence if $E_r$ was being generated as per the model. The above considerations lead us to the conclusion that in the present experiment $E_r \times B_z$ is not the mechanism for the generation of the azimuthal return current.

As was mentioned earlier, the rotating electron beam induced diamagnetic signal does not show any gross oscillatory behaviour of the plasma in the density range $10^{11}$–$10^{13}$ cm$^{-3}$. Similar results have been reported by Kapetanakos *et al* (1975a) and Roberson (1978). In these two experiments, only when the plasma density is above $3 \times 10^{13}$ cm$^{-3}$, the magnetosonic modes were observed. Further, the theoretical model (Molvig and Rostoker 1977a) predicts that the magnetosonic mode will be critically damped if

$$v_e^2 \geqslant 4\, W_{LH}^2 \left(1 + \frac{W_p^2}{k^2 c^2}\right)$$

where $v_e$ is the plasma collision frequency, $W_{LH}$ is the lower hybrid frequency, $W_p$ is the plasma frequency and $k = 2\pi/a$, $a$ is the beam radius.

It is evident from the above expression that the magnetosonic mode will be critically damped at low plasma density while oscillations can be excited only above a certain plasma density, as is confirmed by the present and earlier experiments.

The present experiment has shown that the azimuthal current layer generated by the beam passage through the plasma, decouples itself from the ends of the chamber and persists inside the mirror after the beam has left the mirror. This phenomenon has not been observed in any of the earlier experiments. The main difference between the earlier and the present experiment is that earlier experiments have been performed in uniform fields, with field lines extending axially and in contact with the end walls. In this configuration the axial drift of the electrons under the influence of the induced $E_z$ would short out the electric field, necessary to sustain the azimuthal return currents. In our experiment, the presence of the mirror field would inhibit the easy electron flow to the walls. This is confirmed in the present experiment, where 1 $\mu$sec long diamagnetic signal is observed only with the mirror field, and when the mirror ratio is reduced, the same signal decays in 200 nsec.

The observed shrinking of the azimuthal current layer in the axial direction could be explained by the laws of electrodynamics, whereby the ponderomotive force acting on a current carrying conductor will always be such that it will tend to increase the inductance of the conductor. Applying this analogy, the azimuthal current layer, as a result of the ponderomotive force acting on them, contracts axially.

### 6.3 *Field reversed configuration*

The physical mechanism for the formation of observed field reversed configuration can be understood as follows. The rotating relativistic electron beam is passed through a flux-conserving cylinder containing neutral gas in which is embeded a uniform, external

axial magnetic field $B_0$. Initial conductivity of neutral gas is negligible so that the self field of the beam permeates the gas, and thus ionises it and produces an axial magnetic field opposed to the sense of the external magnetic field. The self-magnetic field is large enough to cause field reversal (*i.e.* $\Delta B_z \geqslant -2B_0$). Then the beam heats the plasma and renders it conducting such that when the beam leaves, it creates comparable induction currents so that the field reversal persists with the aid of the plasma current. The currents decay by internal resistivity and/or particle flow to the walls.

A compact toroid geometry, which is an axisymmetric magnetic confinement system where poloidal ($B_z$) field lines are closed and encircle the plasma while toroidal field ($B_\theta$) is trapped within the plasma, can be formed from the observed field reversed configuration by reconnecting the parallel-antiparallel magnetic field lines at the two ends. The field lines can be reconnected by producing a very fast rising (rise time $\approx$ 100 nsec), long duration (few $\mu$sec) magnetic field in the direction of the initial field. It is expected that during the phase of magnetic field line reconnection most of the axial current will close on the plasma surface. It is planned to dissipate the rest of the axial current by means of an appropriate resistive liner.

## 7. Conclusions

Experimental studies on interaction of a rotating relativistic electron beam with a plasma trapped in a magnetic mirror and on generation of field-reversed configuration have been carried out. Specifically, the rotating electron beam propagation characteristics and magnetic response of the plasma and neutral gas to the beam are investigated in detail.

The propagation of the rotating beam is of magnetic diffusion type, when the plasma density lies in the range $10^{11}$–$10^{13}$ cm$^{-3}$. In this density regime, no radial oscillations of the plasma are observed. The rotating electron beam induces axial and azimuthal return currents in the plasma. The experimental results suggest that the azimuthal return current is of resistive nature rather than drift type. In earlier rotating beam plasma experiments (Kapetanakos *et al* 1975a; Roberson 1978), the diamagnetic loop signal was attributed to plasma heating. However, the present experimental studies indicate that by and large the azimuthal return current diamagnetism contributes to the loop signal. The spatial and temporal variation of the azimuthal return currents observed has shown that the return current layer is trapped in the magnetic mirror and mirror field plays an important role in the formation of the trapped return current layer.

A field-reversed configuration has been formed by rotating relativistic electron beam when injected into neutral gas. We have observed field reversal up to three times the initial field *i.e.* change in the magnetic field on the axis of symmetry of 1·5 kG. The observed configuration has a length of 100 cm. The experimental work on formation of compact toroid from field reversed configuration is in progress.

## References

Andrew M L, Daviation H, Fleischmann H H, Kusse B, Kribel R E and Nation J A 1971 *Phys. Rev. Lett.* **27** 1428

Armstrong W T, Linford R K, Lipson J, Platts D A and Sherwood E G 1981 *Phys. Fluids* **24** 2068

Bagratashoili V N, Knyazev I N, Kudryartsev Yu A and Letikhov V S 1973 *Opt. Commun.* **9** 135

Chu K R, Kapetanakos C A and Clark R W 1975 *Appl. Phys. Lett.* **27** 185
Chu K R and Rostoker N 1974 *Phys. Fluids* **17** 813
Es'Kov A G, Kurtmullaev R Kh, Kreshdruk A P, Laukhain Ya N, Malyutin A I, Markin A I, Martyushov Yu S, Moronov B N, Orlov M M, Proshletsov A P, Semenov V N and Sosunov Yu B 1978 VII *Conf. on Plasma Physics and Controlled Fusion* Vol. II 187
Graybill S E and Uglum J R 1970 *J. Appl. Phys.* **41** 230
Jain K K, John P I, Punithavelu A M and Rao P P 1980 *J. Phys. E* **13** 928
Jain K K and John P I 1981 *Proc. Indian Acad. Sci. (Engg. Sci.)* **4** 75
Jain K K 1982, Ph.D. Thesis, Physical Research Laboratory
Jarboe T R, Henins I, Hoider H W, Lindford R K, Marshall J, Platts D A and Sherwood A R 1980 *Phys. Rev. Lett* **45** 1264
Kapetanakos C A, Black W M and Chu K R 1975a *Phys. Rev. Lett.* **34** 1156
Kapetanakos C A, Black W M and Striffler C D 1975b *Appl. Phys. Lett.* **26** 368
Molvig K and Rostoker N 1977a *Phys. Fluids* **20** 494
Molvig K and Rostoker N 1977b *Phys. Fluids* **20** 504
Nation J A 1970 *Appl. Phys. Lett.* **21** 491
Nebenzahl I 1973 *Plasma Phys.* **15** 1149
Oswald R B, Eisen R A and Conrad E E 1966 *IEEE Trans. Nucl. Sci.* **NS-13** 229
Roberson C W 1978 *Nucl. Fusion* **18** 1693
Roberson C W, Tzach D and Rostoker N 1978 *Appl. Phys. Lett.* **32** 214
Rej D 1981 Ph.D. Thesis, Cornell University
Schmidt G 1962 *Phys. Fluids* **5** 994
Sethian J D, Gerber K A, Hammer D A, Spector D N and Robson A E 1978a *Phys. Fluids* **21** 1227
Sethian J D, Gerber K A, Spector D N and Robson A E 1978b *Phys. Rev. Lett.* **41** 798
Sethian J D, Gerber K A and Robson A E 1982 *NRL Memorandum Report* No. 4932
Striffler C D and Kapetanakos C A 1975 *J. Appl. Phys.* **46** 2509